

Optically detected electron-nuclear double resonance of epitaxial GaN

E. R. Glaser, T. A. Kennedy, W. E. Carlos, J. A. Freitas, Jr., A. E. Wickenden,
and D. D. Koleske

Naval Research Laboratory, Washington, DC 20375-5347

(Received 10 October 1997)

Optically detected electron-nuclear double resonance (ODENDOR) experiments at 24 GHz performed on a set of GaN epitaxial layers grown on Al_2O_3 substrates reveal $^{69,71}\text{Ga}$ signals with quadrupole splittings that reflect the crystal structure and degree of local strain. Searches were made between 1.5 and 140 MHz on both the effective-mass (EM) donor and deep defect resonances revealed from optically detected magnetic resonance (ODMR) studies of the 2.2-eV "yellow" emission bands. Strong ^{69}Ga and ^{71}Ga lines were found between 7 and 14 MHz on the EM donor resonance from two high-resistivity films ($n \leq 1 \times 10^{16} \text{ cm}^{-3}$), and are attributed to neighboring $^{69,71}\text{Ga}$ lattice nuclei. These resonances are split by the local electric-field gradients through the nuclear quadrupole interaction. The quadrupole splittings of 2.16 ± 0.08 and 2.40 ± 0.05 MHz found for ^{69}Ga in these samples are 15–25 % smaller than those reported for a free-standing bulk platelet and for a bulk powder. Similar signals were not observed on the EM-donor lines from two *n*-type GaN layers with $n \geq 3 \times 10^{16} \text{ cm}^{-3}$. These concentration-dependence results reveal the ENDOR mechanisms in GaN. ODENDOR was not found on the deep-defect ODMR. Possible reasons for the absence of signals are presented. [S0163-1829(98)00216-1]

I. INTRODUCTION

The roles of residual defects (both point and extended) and dopants in the electrical and optical activity of GaN-based structures are currently under intense investigation. Evidence of the existence of donors and acceptors with either effective-mass (EM) or deep character (for undoped, Si-doped, and Mg-doped GaN films) has been reported by many groups employing a variety of techniques, including Hall-effect measurements,^{1,2} photoluminescence (PL) spectroscopy,³ electronic Raman scattering,⁴ and magnetic-resonance techniques such as electron paramagnetic resonance (EPR) (Refs. 5 and 6) and optically detected magnetic resonance (ODMR).^{7–10} Evidence of extended defects such as line defects in GaN epitaxial layers grown on sapphire (Al_2O_3) or 6H-SiC substrates has been revealed by high-resolution transmission electron microscopy measurements.^{11–13} Typical dislocation densities are between 10^7 and 10^{10} cm^{-2} , and arise from both the lattice constant mismatch and the difference in thermal-expansion coefficients between the film and substrate. These studies are important for the improvement and further development of short-wavelength ($\lambda \sim 190\text{--}450 \text{ nm}$) emitters^{14,15} and detectors,¹⁶ and high-power-high-temperature electronic devices such as heterojunction field-effect transistors^{17,18} fabricated from III-nitride semiconductors.

Several issues remain with regard to the character of these residual defects and dopants in GaN. These include the chemical identities, binding energies, locations, and effects of the local environment. With regard to the latter, a high degree of electron-nuclear hyperfine interaction in GaN is expected due to the host nuclei (i.e., $^{69,71}\text{Ga}$ and ^{14}N) having finite nuclear spin. In addition, the electric-field gradients (EFG's) that arise from both the wurtzite crystal structure and the local strain fields near dislocations are sensed by the defect nuclei with $I > \frac{1}{2}$ and by the host nuclei (which all

have $I > \frac{1}{2}$) through the nuclear quadrupole interaction.

Defect-related hyperfine and quadrupolar interactions in GaN have been explored recently by two groups using combined electron-nuclear resonance techniques. One group¹⁹ employed optically detected electron-nuclear double resonance (ODENDOR) on a single, undoped film. Fairly weak $^{69,71}\text{Ga}$ ODENDOR was detected on the EM donor resonance found on the 2.2-eV yellow emission band. These spectra were tentatively assigned to Ga interstitials (Ga_i). Another group²⁰ detected Overhauser shifts on the shallow-donor EPR found from an undoped platelet, with $n_{300\text{K}} \sim 5 \times 10^{16} \text{ cm}^{-3}$. Very sharp and strong NMR lines attributed to the host $^{69,71}\text{Ga}$ and ^{14}N nuclei were revealed, and high-precision values for the electric-field gradients at these sites were determined from the quadrupole splittings.

In this work we have performed ODENDOR studies of three undoped and one lightly Si-doped GaN epitaxial layers grown on sapphire substrates by organometallic chemical-vapor deposition (OMCVD). Searches were made on both the EM donor (with $g \sim 1.950$) and deep defect (with $g \sim 1.992$) ODMR found on the 2.2-eV PL bands.

The main results of this work derive from the observation of very strong ODENDOR signals between 7 and 14 MHz on the EM donor resonance found on the 2.2-eV emission bands from the two undoped samples with high resistivity (HR). We attribute these lines to $^{69,71}\text{Ga}$ lattice nuclei that sense the wurtzite-crystal field and local strains through the nuclear quadrupole interaction. In addition, we infer that these nuclei are coupled to the residual EM donors through a weak, unresolved hyperfine interaction. This ODENDOR was not found on similar EM donor ODMR from the as-grown (*n*-type) and Si-doped GaN films with $n \geq 3 \times 10^{16} \text{ cm}^{-3}$. The quadrupole splittings found for the $^{69,71}\text{Ga}$ nuclei differ from those reported for a strain-free, 220- μm -thick platelet and for a bulk powder. Finally, ODENDOR did not reveal strong signals between 1.5 and 140 MHz on the

TABLE I. GaN epitaxial layers investigated in this work.

Sample designation	Thickness (μm)	Doping	Transport properties (300 K)
No. 1 (#50209)	3.5	None	Highly Resistive ($\rho \sim 10^{10} \Omega \text{ cm}$)
No. 2 (#60611)	2.7	None	Highly Resistive ($\rho \sim 10^{10} \Omega \text{ cm}$)
No. 3 (GaN #1)	5.6	None	$n \sim 3 \times 10^{16} \text{ cm}^{-3}$
No. 4 (#51031)	2.7	Si	$n \sim 6 \times 10^{16} \text{ cm}^{-3}$

deep-defect ODMR feature. Possible reasons for the lack of signals are presented.

The paper is divided into six sections. Section I is the introduction. In Sec. II, the optically detected electron-nuclear double-resonance spectrometer is described, including some details of the photoluminescence and optically detected magnetic-resonance experiments that form the background for the present work. In addition, a table of sample parameters is provided, including results of room-temperature electrical transport measurements. The spin Hamiltonian employed to model the electron- and nuclear-spin resonances observed in these studies is described in Sec. III. Also, the resonance conditions for electron and nuclear spin-flip transitions that derive from this spin Hamiltonian are provided. The results of the PL, ODMR, and ODENDOR experiments performed on the undoped and lightly Si-doped GaN films are given in Sec. IV. Analysis and discussion of the results are given in Sec. V, including a comparison with other recent electron-nuclear double-resonance experiments performed on GaN, and with previous ENDOR studies of other III-V semiconductors (in particular, bulk GaP crystals doped with S or Te). A summary and overall conclusions are provided in Sec. VI.

II. EXPERIMENTAL BACKGROUND

The experiments were performed on four GaN epitaxial layers grown on (0001)-oriented Al_2O_3 substrates by OMCVD. The films have the wurtzite-crystal structure. AlN or GaN nucleation layers ($\sim 250\text{--}400 \text{ \AA}$) were deposited on the substrates prior to the growth of the GaN films. One of the films was lightly doped with Si using disilane (Si_2H_6). Additional details of the growth are given elsewhere.²¹ The layer thicknesses, conductivity type, and carrier concentration determined from room-temperature Hall-effect measurements are given in Table I. The layer thicknesses determined for some of these films from infrared reflectivity measurements were in very good agreement with the nominal values derived from the growth rates. As noted in Table I, two of the films (Nos. 1 and 2) investigated in this work are highly resistive at 300 K, with breakdown voltages greater than 1000 V. The other two layers (Nos. 3 and 4) were found to be n type, with carrier concentrations in the low- to mid- 10^{16}-cm^{-3} range.

For PL at low temperatures including the band edge, the samples were excited with above-band-gap radiation provided by the 325-nm line of a HeCd laser at a power density of $\sim 40 \text{ W/cm}^2$. The emission from 1.8 to 3.6 eV was analyzed by a 0.85-m double-grating spectrometer, and detected with a UV-enhanced GaAs photomultiplier tube.

The ODMR was detected as the change in the total inten-

sity of the broad 2.2-eV emission which was coherent with on-off modulation ($\sim 270 \text{ Hz}$) of 50 mW of microwave power at 24 GHz. The samples were studied under pumped-helium conditions ($\sim 1.6 \text{ K}$) in a commercial cryostat with optical access. The dc magnetic field was provided by a 9-in. electromagnet with a maximum field of 1.1 T. For the ODMR, the PL was continuously excited by the 351.1-nm line from an Ar^+ -ion laser with power densities near 140 mW/cm^2 . The emission was detected by a room-temperature, UV-enhanced Si photodiode. UV and visible cutoff filters were placed in front of the detector to spectrally isolate the 2.2-eV yellow band. Strong ODMR signals ($\Delta I/I \sim 0.5\text{--}1\%$) were observed from these samples for such excitation conditions. In addition, the PL below 3.4 eV was analyzed at 1.6 K by a 0.25-m double-grating spectrometer, and detected by the same Si photodiode used for the ODMR studies.

The ODENDOR experiments were carried out in the TE_{011} microwave cavity, which has four parallel Cu wires (0.023-in. diameter) running vertically and connected outside the cavity to produce a two-turn rf coil.²² The rf current was delivered to the coil from the top of the insert by a 1-m-long, small-diameter coaxial (50- Ω) line. The rf was generated by a Wavetek Model 2410 synthesizer and amplified by a ENI 550L amplifier. Typical rf powers used in these studies were $\sim 10 \text{ W}$. The ODENDOR was performed with the dc magnetic field fixed at the value for an electron-spin resonance of the optically excited state. The best signal-to-noise ratio was obtained with cw microwave radiation, and on-off amplitude modulation of the rf. Searches for ODENDOR were made between 1.5 and 140 MHz.

III. SPIN HAMILTONIAN AND CONDITIONS FOR RESONANCE

The ODMR and ODENDOR spectra were analyzed with the following spin Hamiltonian:²³

$$H = H_e + H_n + H_{e-n}, \quad (1)$$

with

$$H_e = \mu_B g_e \mathbf{S} \cdot \mathbf{B}, \quad (2)$$

$$H_n = -\mu_N g_n \mathbf{I} \cdot \mathbf{B}, \quad (3)$$

$$H_{e-n} = \mathbf{I} \cdot \mathbf{A} \cdot \mathbf{S} + \mathbf{I} \cdot \mathbf{Q} \cdot \mathbf{I}, \quad (4)$$

where H_e is the electronic Zeeman term, H_n is the nuclear Zeeman term, and H_{e-n} is comprised of two field-independent terms. In Eqs. (2)–(4), μ_B and μ_N are the electronic (Bohr) and nuclear magnetons, g_e and g_n are the elec-

tronic and nuclear g values, \mathbf{S} and \mathbf{I} are the electronic and nuclear spins, \mathbf{B} is the applied dc magnetic field, \mathbf{A} is the electron-nuclear (hyperfine) interaction tensor, and \mathbf{Q} is the quadrupole tensor. The nuclei include both the defect nucleus (which produces the central hyperfine interaction if it has a nuclear moment) and the host-lattice nuclei (which produce the ligand or superhyperfine interactions). The nuclear quadrupole interaction is nonzero if $I > \frac{1}{2}$, and the symmetry at the particular nucleus is lower than cubic; such as is the case in GaN with wurtzite crystal structure.

In the simple case of an electron with $S = \frac{1}{2}$ and a nucleus with $I = \frac{1}{2}$, the condition for an electronic spin flip ($\Delta m_s = \pm 1$, $\Delta m_l = 0$), with g and \mathbf{A} isotropic, is given by

$$(h\nu_0)^\pm = g_e \mu_B B_{\text{res}} \pm A/2, \quad (5)$$

where $(h\nu_0)$ is the quantum of energy absorbed. The second (hyperfine) term gives rise to a resolved structure in the ODMR spectra in favorable cases or, oftentimes, is an important source of broadening, especially for ODMR of defects in III-V semiconductors where all the lattice nuclei have $I > 0$.

The resonance condition for nuclear spin flips in ENDOR experiments ($\Delta m_s = 0$, $\Delta m_l = \pm 1$) for an electron spin with $S = \frac{1}{2}$ and for hyperfine (\mathbf{A}) and quadrupole (\mathbf{Q}) tensors, with axial symmetry, is²³

$$h\nu^\pm(m_q, \theta, \theta') = \left| \frac{1}{2} [a + b(3 \cos^2 \theta - 1)] + g_n \mu_N B_0 + 3(m_q)q(3 \cos^2 \theta' - 1) \right|, \quad (6)$$

where B_0 is the fixed dc magnetic field (typically at or near the resonance condition for an electron spin flip in ENDOR), a and b are the isotropic and anisotropic parts of the hyperfine tensor (\mathbf{A}), q is the quadrupole interaction parameter, θ and θ' are the polar angles of the dc magnetic field with respect to the principal axes of the hyperfine (\mathbf{A}) and quadrupole (\mathbf{Q}) tensors, and $m_q = (1/2)(m_l + m_{l'})$, where m_l and $m_{l'}$ are the magnetic quantum numbers of the nuclear states between which the nuclear-spin transitions occur. The third term in Eq. (6) is a nonzero for defect or host nuclei with $I > \frac{1}{2}$ in a symmetry lower than cubic. For example, for nuclei such as ^{69}Ga or ^{71}Ga with spin $I = \frac{3}{2}$, $m_l = -\frac{3}{2}, -\frac{1}{2}, +\frac{1}{2}$, and $+\frac{3}{2}$, the quadrupole interaction produces three lines labeled by $m_q = -1, 0$, and $+1$ with relative intensities of 3:4:3.²⁴ In the absence of second-order corrections, the lines are degenerate for $\theta' = 54.7^\circ$.

IV. RESULTS

A. Photoluminescence

The photoluminescence at 6 K from the four samples is shown in Fig. 1. Five distinct bands are revealed in these spectra. One recombination is common to all the samples, while the others are particular to two classes of samples.

The strongest emission from all four samples is a sharp peak (the full width at half maximum is $\sim 3\text{--}5$ meV) at an energy between 3.472 and 3.487 eV. The dominant component of the band-edge PL from the two HR GaN films (Nos. 1 and 2) has been attributed to free excitonic recombination (labeled FX) from temperature-dependent PL studies.²⁵ The band-edge PL emission from the two n -type films (Nos. 3

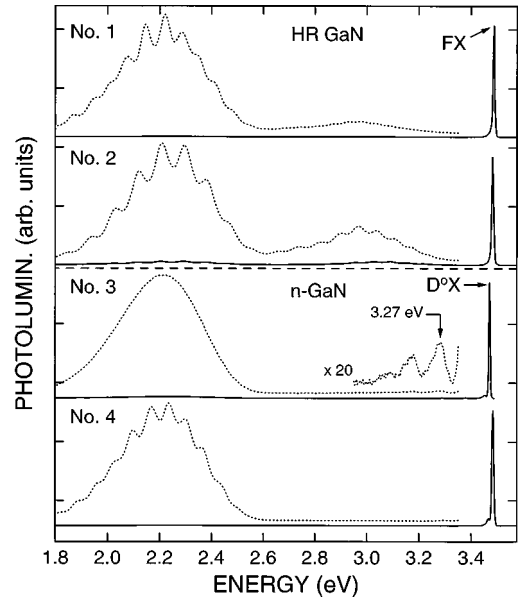


FIG. 1. PL spectra obtained from two high-resistivity (HR) and two n -type GaN films at ~ 6 K. The curves displaced vertically show the PL < 3.4 eV under excitation conditions similar to those employed for the ODMR and ODENDOR studies. The periodic structure on the 3.0- and 2.2-eV emission bands is due to multiple reflections in the GaN layers.

and 4) was assigned to excitons bound to neutral donors (labeled D^0X). A third PL band with a zero-phonon line at 3.27 eV and a series of LO-phonon replicas at lower energies is seen for sample No. 3. This emission was assigned²⁶ to shallow-donor (SD)–shallow-acceptor (SA) pairs, and is most easily observed at low excitation power densities. The absence of SD-SA emission, and the observation of strong free-excitonic recombination from the HR films suggests that the residual numbers of shallow donors and acceptors are fewer than 10^{16} cm^{-3} .

Two broad emission bands at 2.2 and 3.0 eV with Gaussian line shapes and linewidths of ~ 400 meV are also found from the HR samples. These bands are much weaker in amplitude than the band-edge emission observed from all the films under light excitation densities of $\sim 40 \text{ W/cm}^2$. The dotted curves in Fig. 1 indicate the relative strengths of the deep bands expanded for comparison under the same experimental conditions employed for the ODMR studies.

The broad band at 3.0 eV has only been observed from the HR GaN films. Other groups⁸ only found this band from GaN films that exhibit some evidence of free excitonic recombination at low temperature. The ODMR found on the 3.0-eV band was the subject of a preliminary report.²⁷

The broad emission at 2.2 eV (commonly referred to as the “yellow” band) is found from all four samples. The 2.2-eV band has been found to some degree of strength from most undoped, n -type GaN layers grown at Naval Research Laboratory and for similar samples grown by other laboratories. ODMR and ODENDOR on the 2.2-eV band will be discussed below.

B. ODMR on 2.2-eV PL Band

ODMR spectra were obtained at 24 GHz on the 2.2-eV emission bands for all four samples with $\mathbf{B} = 55^\circ$ from c (see

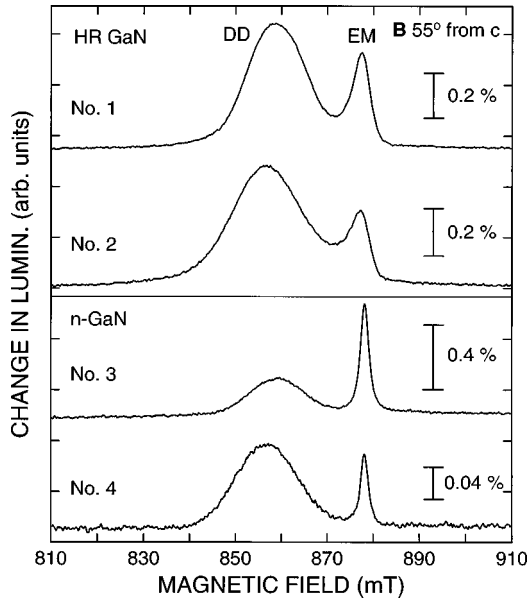


FIG. 2. ODMR spectra found at 24 GHz on the 2.2-eV emission bands from two HR and two *n*-type GaN layers with $\mathbf{B}=55^\circ$ from *c*. Magnetic resonance features labeled EM (assigned to effective-mass donors) and DD (assigned to deep defects) are observed in all these samples.

Fig. 2). Two luminescence-increasing resonances, labeled EM and DD (deep donor), are dominant. Similar spectra from undoped, *n*-type GaN were reported by other groups.^{8–10}

The EM-signal is sharp with $g \sim 1.951$ for this field orientation. This feature was assigned to effective-mass donor states.^{5,7} We emphasize here the changes in both the shape and linewidth of the EM signal between the two *n*-type GaN layers and the two HR GaN films. In particular, the line from the *n*-type GaN films (Nos. 3 and 4) can be fit by a Lorentzian with a full width at half maximum (FWHM) of ~ 2.1 mT. However, the line from the two HR GaN films (Nos. 1 and 2) is best fit with a Voigt function (i.e., a

convolution of Lorentzian and Gaussian line shapes) with a FWHM of ~ 4 mT. A summary of the parameters for these EM lines is given in Table II.

The signal labeled DD is broad (a FWHM of ~ 13.5 – 18 mT) with $g \sim 1.991$. This resonance was assigned to deep donors located in the upper half of the band gap based on its resonance parameters, and a capture-recombination model proposed for the 2.2-eV band.^{7,10} In another interpretation, this resonance is attributed to deep donors in the lower half of the band gap based on a different model for the recombination process.⁹

An additional weaker line at ~ 874 mT is needed to fit the spectra for the two HR films. This resonance is partially resolved in 35-GHz data, and will be discussed in a future paper.²⁸

C. ODENDOR on EM and DD resonances

ODENDOR was studied between 6 and 14 MHz on the EM resonance (i.e., for $B_{\text{res}}=877$ mT) from samples Nos. 1–4 with $\mathbf{B}=55^\circ$ from *c* (see Fig. 3). The same power density for light excitation (~ 140 mW/cm²) and rf power (~ 10 W) were employed for each sample. Several features are evident. First, two strong lines with similar amplitudes were found from the two high-resistivity GaN layers at the free nuclear Larmor frequencies of ⁶⁹Ga and ⁷¹Ga. The ODENDOR is ~ 3.0 – 5.5×10^{-4} as a fraction of the 2.2-eV PL and ~ 10 – 15% as a fraction of the EM ODMR intensities. Second, examination of the line shapes indicates both broad and sharp components. Third, no ODENDOR was found from the two *n*-type films.

ODENDOR for sample No. 1 is shown for two orientations of the applied magnetic field in Fig. 4. We emphasize the triplet (labeled $m_q = -1, 0,$ and $+1$) that is resolved near 9.0 MHz with $\mathbf{B} \perp c$. The splitting between $m_q = -1$ and $+1$ (determined from fits discussed in Sec. V) is $\sim 1.20 \pm 0.02$ MHz for sample No. 1, and $\sim 1.08 \pm 0.04$ MHz for sample No. 2. ODENDOR obtained for additional magnetic-field orientations reveals that the splitting near 9.0 MHz is

TABLE II. Summary of shallow donor magnetic resonance parameters for HR and *n*-type GaN films studied in this work with $\mathbf{B}=55^\circ$ from *c* and comparison to values reported from other experiments (*G*, Gaussian; *L*, Lorentzian).

Sample	<i>g</i> value	Line shape	FWHM (mT)	Technique
No. 1 (HR GaN)	1.9506 ± 0.0004	<i>L/G</i>	3.9	ODMR (this work)
No. 2 (HR GaN)	1.9511 ± 0.0004	<i>L/G</i>	4.2	
(<i>n</i> -type GaN) No. 3	1.9494 ± 0.0002	<i>L</i>	2.2	
No. 4 (<i>n</i> -type GaN)	1.9495 ± 0.0002	<i>L</i>	2.0	
GaN/Al ₂ O ₃	$g_{\parallel} = 1.9513$	<i>L/G</i>	~ 5	ODMR (Koschnick <i>et al.</i> ^a)
220 μm thick GaN platelet	$g_{\parallel} = 1.9503 \pm 0.0001,$ $g_{\perp} = 1.9483 \pm 0.0001$	<i>L</i>	0.5	EPR (Denninger and Reiser ^b)

^aReference 19.

^bReference 20.

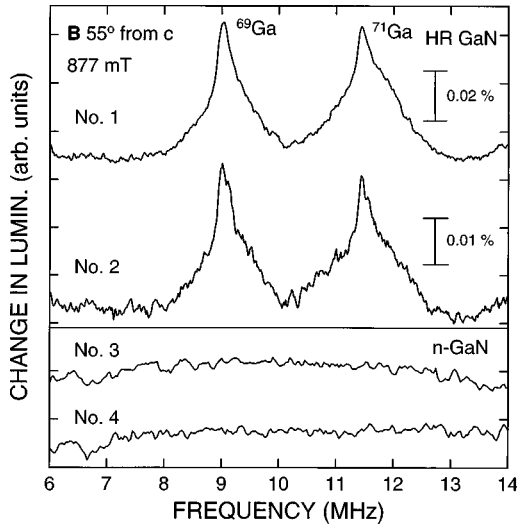


FIG. 3. ODENDOR spectra obtained on the EM donor resonance ($B_{\text{res}}=877$ mT) observed from the four samples with $\mathbf{B}=55^\circ$ from c . Strong NMR signals are only observed from the HR GaN films. The peak positions are very close to the free nuclear Larmor frequencies of ^{69}Ga and ^{71}Ga .

proportional to $(3 \cos^2 \theta' - 1)$, where θ' is the angle between \mathbf{B} and the c axis. Though not well resolved, there is also a hint of three-component structure near 11.4 MHz with $\mathbf{B} \perp c$. This splitting is roughly 63% (the ratio of the $^{71}\text{Ga}/^{69}\text{Ga}$ quadrupole moments) of that found for the three lines near 9.0 MHz. The amplitudes of the three resolved lines seen near 9.0 MHz, with $\mathbf{B} \perp c$, are approximately equal. In addition, the amplitude of the signal near 11.4 MHz is ~ 1.6 times larger than that found for the lines near 9.0 MHz. The relative intensities observed from sample No. 2 exhibit similar behavior.

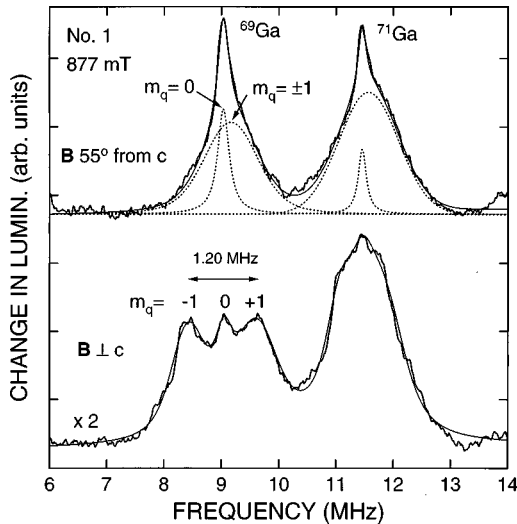


FIG. 4. ODENDOR spectra found on the EM donor line from HR GaN film No. 1 with $\mathbf{B}=55^\circ$ from c (top half) and $\mathbf{B} \perp c$ (bottom half). The major features of these spectra can be understood using a first-order quadrupole analysis with second-order corrections (see text). The thin solid lines are fits to the spectra as described in the text. The individual components (labeled $m_q=0$ and ± 1) of the fit to the ODENDOR spectrum obtained with $\mathbf{B}=55^\circ$ from c are shown as the dotted curves (see also Table III).

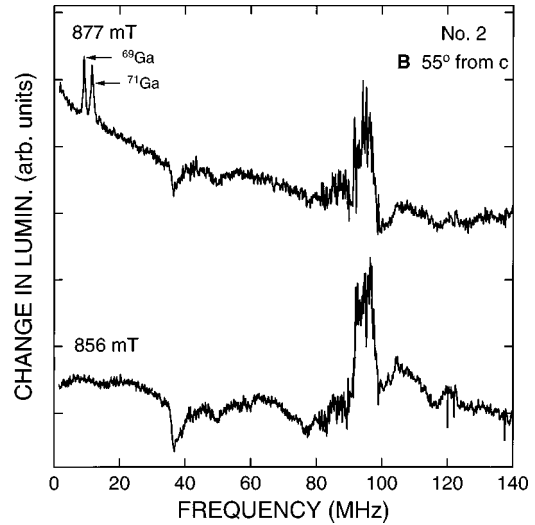


FIG. 5. ODENDOR spectra found between 1.5 and 140 MHz on the EM ($B_{\text{res}}=877$ mT) and deep defect ($B_{\text{res}}=856$ mT) ODMR from sample No. 2 with $\mathbf{B}=55^\circ$ from c . The positive and negative signals between ~ 35 and 140 MHz are due to resonances in the rf system (see text).

Similar ODENDOR spectra were obtained from an n -type GaN layer by Koschnick *et al.*¹⁹ However, in contrast to the present work, the lines were very weak, only $\sim 2 \times 10^{-5}$ of the total luminescence. Also, Denninger *et al.*²⁰ recently observed sharp and strong ^{69}Ga and ^{71}Ga NMR with similar splittings and ^{14}N NMR from Overhauser-shift experiments on the shallow-donor EPR from a $220\text{-}\mu\text{m}$ GaN platelet.

ODENDOR was studied from 1.5 to 140 MHz on the EM ($B_{\text{res}}=877$ mT) and deep-defect ($B_{\text{res}}=856$ mT) ODMR from sample No. 2 with $\mathbf{B}=55^\circ$ from c (see Fig. 5). The excitation power density and rf power conditions were kept constant. Several features are evident. First, the ODENDOR from ^{69}Ga and ^{71}Ga is not found on the deep-defect ODMR. Second, no evidence was found of the ^{14}N NMR expected at ~ 2.7 MHz. This contrasts with the results of Denninger *et al.*,²⁰ but agrees with the results of Koschnick *et al.*¹⁹ Third, no ENDOR could be definitively observed in this frequency range except those lines found between 6 and 14 MHz on the EM resonance. The additional luminescence-increasing and -decreasing features observed at higher frequencies are due to resonances in the rf system. These resonances cause large rf ground currents to flow in the K -band microwave cavity and lead to large variations in the ODMR, especially between 35 and 100 MHz in the present experiments. The size of the background observed on the ODMR at 856 mT compared to that found on the ODMR at 877 mT scales with the relative amplitudes of these lines (see Fig. 2). Improvements are underway to eliminate this background so that additional ODENDOR can be revealed.

V. DISCUSSION

A. Assignment of lines

The ODENDOR can be described using a first-order quadrupole analysis with second-order corrections.²⁴ We assign the NMR to $^{69,71}\text{Ga}$ lattice nuclei coupled to the residual EM donors by a weak hyperfine interaction [i.e., a/h , b/h

≤ 1 MHz in Eq. (6)] because no resolved lines are detected with large hyperfine interactions. First, the wurtzite-crystal structure produces a finite electric-field gradient at the nuclear sites. This electric-field gradient is sensed by the $^{69,71}\text{Ga}$ nuclei through the quadrupole interaction [second term in Eq. (4)]. Second, random strain fields from the dislocations lead to additional field gradients, and are sensed by the Ga nuclei.

As discussed in Sec. III, in the presence of a nonzero quadrupole interaction, three lines (characterized by quantum numbers $m_q = -1, 0,$ and $+1$) are expected for isotopes with $I = \frac{3}{2}$. In a first-order analysis and with $a/h, b/h \leq 1$ MHz based on the linewidths, the $m_q = 0$ line will occur at the Larmor frequency (i.e., $\nu = \nu_L \equiv 1/h |g_n \mu_N B_0|$) of the nuclear species) for all magnetic-field orientations. The three lines will be degenerate for $\mathbf{B} = 54.7^\circ$ from c . In addition, the maximum splitting between the $m_q = -1$ and $+1$ lines occurs for $\mathbf{B} \parallel c$ ($\theta' = 0^\circ$), while half this splitting is expected for $\mathbf{B} \perp c$ ($\theta' = 90^\circ$). These splittings are clearly observed for the ^{69}Ga nuclei with $\mathbf{B} \perp c$ (bottom half of Fig. 4). Since the quadrupole splitting is proportional to the quadrupole moment (Q), the splitting for the ^{71}Ga nuclei is expected to be $\sim 63\%$ of that for the ^{69}Ga nuclei, since $Q(^{71}\text{Ga})/Q(^{69}\text{Ga}) = 0.63$ (Ref. 29). This splitting is not resolved since the individual linewidths are of the order of the expected splitting (i.e., ~ 0.7 MHz).

We assign the strong NMR to $^{69,71}\text{Ga}$ nuclei from neighboring shells coupled to the EM donors by weak (≤ 1 MHz) hyperfine interactions. The weakness of the hyperfine interaction between the donor wave function and the nearby $^{69,71}\text{Ga}$ shells in GaN can be understood from an examination of the ionization energies, Bohr radii, and hyperfine parameters found from ENDOR of S- and Te-doped GaP crystals.³⁰ In that work, the hyperfine parameters and their symmetries for several groups of neighboring nuclei were found from ENDOR of the S and Te shallow-donor ESR signals. Most noteworthy, the isotropic constant, a , for the first shell of ^{69}Ga is ~ 27.7 MHz for the S donors whose $E_D \sim 100$ meV and more than a factor of 2 smaller (i.e., ~ 12.5 MHz) for the slightly shallower Te donors with $E_D \sim 90$ meV. The corresponding Bohr radii of these donors is ~ 7 Å. NMR was also observed at the Larmor frequencies of the lattice nuclei (i.e., ^{69}Ga , ^{71}Ga , and ^{31}P) from other neighbor shells with small ligand hyperfine interactions (≤ 1 MHz). For GaN, the binding energy for shallow donors is ~ 30 meV (Ref. 3) with a Bohr radius of ~ 25 Å. Thus the much larger extent of the wave function estimated for EM donors in GaN compared to the donors in GaP suggests that the near-neighbor hyperfine interaction associated with the $^{69,71}\text{Ga}$ lattice nuclei in GaN would be weak (i.e., ≤ 1 MHz). This small hyperfine interaction would contribute to the linewidth of the observed signals. Indeed, the estimate is consistent with the linewidths (i.e., ~ 0.2 – 1.2 MHz) to be discussed in Sec. V B. Finally, the GaN ODENDOR results are similar to those reported³¹ from ODENDOR of shallow donors in ZnSe and CdS crystals for which the Bohr radii (~ 27 – 29 Å) and binding energies (~ 26 – 30 meV) are very close to the values given above for GaN. In particular, NMR was only observed at the Larmor frequencies of the lattice nuclei (i.e., ^{67}Zn , ^{77}Se , $^{111,113}\text{Cd}$, and ^{33}S) with similar line-

TABLE III. Summary of line positions and widths from fits of ODENDOR spectra (see Fig. 4) found on EM donor resonance at $B = 877$ mT for sample No. 1 with (a) $\mathbf{B} = 55^\circ$ from c and (b) $\mathbf{B} \perp c$. Best fits were obtained with Lorentzian line shapes for the $m_q = 0$ quadrupole lines and Voigt line shapes (i.e., mixed Lorentzian/Gaussian character) for the $m_q = \pm 1$ quadrupole lines. Similar parameters were found for sample No. 2.

Assignment	Res. frequency (MHz)	FWHM (MHz)
(a) $\mathbf{B} = 55^\circ$ from c		
^{69}Ga NMR:		
$m_q = 0$	9.03	0.24
$m_q = \pm 1$	9.16	1.22
^{71}Ga NMR:		
$m_q = 0$	11.46	0.17
$m_q = \pm 1$	11.57	1.11
(b) $\mathbf{B} \perp c$		
^{69}Ga NMR:		
$m_q = -1$	8.42	0.72
$m_q = 0$	9.04	0.40
$m_q = +1$	9.62	0.91
^{71}Ga NMR:		
$m_q = -1$	11.07	0.63
$m_q = 0$	11.46	0.61
$m_q = +1$	11.83	0.86

widths as found for the NMR from the HR GaN layers. Small hyperfine interactions (~ 0.5 – 3 MHz) associated with these nuclei were estimated from the NMR linewidths.

B. Analysis of line shapes

The ODENDOR for $\mathbf{B} = 55^\circ$ from c can be fit with the sum of a sharp Lorentzian component (a FWHM of ~ 0.2 MHz) and a Voigt function (i.e., mixed Lorentzian/Gaussian character) with a broader linewidth (a FWHM of ~ 1.2 MHz) as depicted by the dotted curves in Fig. 4. The parameters obtained from this fit are summarized in Table III. We assign the sharp components to the $m_q = 0$ transitions and the broad components to the $m_q = \pm 1$ transitions. We note again that in a first-order quadrupole analysis, all three NMR lines for a particular nuclear species should occur at the Larmor frequency for $\mathbf{B} = 54.7^\circ$ from c . The small shift of the $m_q = 0$ components relative to the $m_q = \pm 1$ lines (0.13 MHz for ^{69}Ga and 0.11 MHz for ^{71}Ga) is evidence of a second-order quadrupole interaction.²⁴ The magnitude of this shift is proportional to the ratio of the square of the quadrupole splitting to the Larmor frequency as described in Ref. 24. The shifts calculated using the quadrupole splittings observed with $\mathbf{B} \perp c$ are 0.16 MHz for ^{69}Ga and 0.05 MHz for ^{71}Ga . The difference between the observed and calculated shifts is approximately equal to the error and will be investigated further.

A reasonable fit was also made to the ODENDOR for $\mathbf{B} \perp c$ using the same line shapes for the $m_q = 0$ and $m_q = \pm 1$ transitions as employed for $\mathbf{B} = 55^\circ$ from c (see Fig. 4). The parameters from this fit are also provided in Table III. The full quadrupole splitting for the ^{69}Ga nuclei deter-

mined from the fit to this spectrum is 2.40 ± 0.05 MHz for sample No. 1 and is 2.16 ± 0.08 MHz for sample No. 2. The electric-field gradients (V_{zz}) at the ^{69}Ga nuclei are determined by multiplying these values by h/eQ , where $Q = 0.168 \times 10^{-28} \text{ m}^2$ (Ref. 29).

As noted previously, the presence of high dislocation densities in these films is expected to lead to electric-field gradients which vary both in magnitude and orientation. This will lead to an inhomogeneous broadening of the $m_q = \pm 1$ lines. In extreme cases, these satellites would broaden beyond observability. The $m_q = 0$ line is not affected by first-order broadening.²⁴

From inspection of the parameters in Table III, the linewidths of the $m_q = \pm 1$ signals observed with $\mathbf{B} = 55^\circ$ from c are larger than the corresponding linewidths with $\mathbf{B} \perp c$. The main contributions to the linewidth with $\mathbf{B} = 55^\circ$ from c are from the distribution in angular orientations of the electric-field gradients revealed through the $3 \cos^2 \theta' - 1$ angular dependence [see Eq. (6), and recall that θ' is the angle between \mathbf{B} and the principal axis of the quadrupole interaction] and from the distribution in the strength of the quadrupole interaction. The linewidths with $\mathbf{B} \perp c$ reflect the smaller distribution in the strength of the quadrupole interaction. Very small changes in frequency from misorientation are expected (again from the $3 \cos^2 \theta' - 1$ angular dependence) for the $m_q = \pm 1$ quadrupole lines with $\theta' \geq 75^\circ$ or $\leq 15^\circ$. Thus we estimate a range of tilt angles for the principal axes of the EFG's of $\sim 5^\circ - 10^\circ$ from the ~ 0.4 -MHz difference in linewidths of the $m_q = \pm 1$ signals with $\mathbf{B} = 55^\circ$ from c and $\mathbf{B} \perp c$.

The peak amplitudes of the three quadrupole lines for both the ^{69}Ga and ^{71}Ga isotopes do not exhibit the expected 3:4:3 ratio²⁴ (see the bottom half of Fig. 4). As discussed above, first-order effects result in a broadening of the $m_q = \pm 1$ lines with the $m_q = 0$ line unaffected. Hence the origin of the reduced intensities observed for the $m_q = 0$ lines is not understood at this time.

C. ENDOR mechanisms

A likely mechanism to account for the luminescence-increasing ODENDOR signals on the EM resonance is that proposed to model the ODENDOR of shallow donors in ZnSe and CdS (Ref. 31). This model is based on the spin-dependent nature of the relaxation and/or recombination processes responsible for the observation of ODMR.^{32,33} In brief, when the ENDOR condition is satisfied [see Eq. (6)], there will be a transfer of excess population from the combined electron-nuclear states for which the donor ODMR condition is not satisfied (due to the presence of the hyperfine interaction) to states for which the condition is met. This, in turn, leads to an increase in the emission.

The dependence of the strength of the GaN ENDOR on carrier concentration reveals aspects of the mechanism of observation. In GaP samples doped with high concentrations of S and Te, such that there is overlap of the donor wave functions, EPR was found³⁴ with Lorentzian line shapes and narrow linewidths. Due to the hopping from one donor site to another in such cases, the ligand hyperfine interaction is averaged out. However, EPR signals with Gaussian line shapes and broad linewidths were found³⁰ with $n \leq 2.5$

$\times 10^{17} \text{ cm}^{-3}$. ENDOR was only observed from these lightly doped GaP crystals. In this regime the donors are isolated and ligand hyperfine interactions remain intact.

In analogy to GaP, Lorentzian line shapes with narrow linewidths (~ 0.5 mT) were observed from EPR of interacting donors in GaN layers⁵ and thick, free-standing platelets with $n \geq 3 \times 10^{16} \text{ cm}^{-3}$ (Ref. 20). As noted in Sec. IV B, Lorentzian ODMR line shapes and narrow linewidths are also found from the conducting films (sample Nos. 3 and 4) investigated in this work (see Fig. 2). Thus, the mixed Lorentzian/Gaussian character and the broad linewidths of the EM donor ODMR from the HR layers (sample Nos. 1 and 2) are consistent with a contribution to the line shapes from hyperfine interactions. This contribution is estimated to be ~ 1.1 mT from a comparison of the linewidths observed at 24 and 35 GHz (Ref. 28). The value is much smaller than that predicted²⁰ from a Monte Carlo calculation of the expected linewidth (~ 10 – 20 mT) in the isolated donor limit due to hyperfine interactions with the lattice nuclei. This discrepancy is not understood at this time.

The higher concentration for observing ENDOR from GaP compared to the concentration for similar observations in GaN (i.e., $\leq 1 \times 10^{16} \text{ cm}^{-3}$) is expected from the smaller Bohr radius in GaP ($\sim 7 \text{ \AA}$) compared to the Bohr radius in GaN ($\sim 25 \text{ \AA}$). The ODENDOR in GaN confirms the recent prediction²⁰ for the concentration regimes where ENDOR and Overhauser-shift ESR would be applicable in GaN.

D. Comparison with other results

The quadrupole splittings for the ^{69}Ga sites in sample Nos. 1 and 2 can be compared to the values from previous ODENDOR,¹⁹ Overhauser-shift NMR,²⁰ and ‘‘magic-angle’’ spinning (MAS) NMR (Ref. 35) experiments (see Table IV). The splittings are all within 25%. This indicates that the dominant contribution to the electric-field gradients derives from the wurtzite-crystal structure. The small differences are attributed to the details of the particular sample and/or measurement technique as discussed below. Also, we note that the errors in the splittings are smaller than the individual differences, and demonstrate the high precision of these magnetic-resonance techniques.

Two points are of particular interest. First, the splittings found for the two HR GaN layers are 15–25 % smaller than the values determined recently from Overhauser-shift experiments²⁰ on a 220- μm , free-standing GaN platelet and from MAS NMR of a powder sample.³⁵ We propose that these differences derive from the degree of residual strain at the lattice nuclei. In particular, the contributions to the local strain from both the lattice constant mismatch and the difference in thermal expansion coefficients between the GaN films and Al_2O_3 substrates are absent in the free-standing platelet and bulk powder. Thus one would expect that the quadrupole splittings for the $^{69,71}\text{Ga}$ nuclei in the GaN layers would differ from those in the ‘‘bulk’’ samples. We note that the MAS NMR technique³⁵ provides an ensemble average of the quadrupole interaction, since all the Ga nuclei contribute to the observed signal. In contrast, the ODENDOR and Overhauser-shift NMR experiments yield an average of the quadrupole interaction only from Ga nuclei within several Bohr radii ($\sim 10 \times$) of the EM donors. Second, the quadru-

TABLE IV. Values of quadrupole splittings for ^{69}Ga determined from ODENDOR spectra with $\mathbf{B} \perp c$ for HR GaN films studied in this work, and comparison to values reported from other experiments. The electric-field gradients (V_{zz}) at the ^{69}Ga nuclei are derived by multiplying these values by h/eQ , where $Q = 0.168 \times 10^{-28} \text{ m}^2$ (Ref. 29).

Sample	$ \nu(m_q = +1) - \nu(m_q = -1) _{\text{max}}$ (MHz)	Technique
No. 1 (HR GaN)	2.40 ± 0.05 MHz	ODENDOR
No. 2 (HR GaN)	2.16 ± 0.08 MHz	(this work)
GaN/ Al_2O_3	2.64 ± 0.08 MHz	ODENDOR (Koschnick <i>et al.</i> ^a)
220 μm thick GaN platelet	2.865 ± 0.015 MHz	Overhauser shift (Denninger and Reiser ^b)
Bulk powder	2.75 MHz	MAS NMR (Han, Timken, and Oldfield ^c)

^aReference 19.

^bReference 20.

^cReference 35.

pole splittings for sample Nos. 1 and 2 differ by $\sim 10\%$. X-ray measurements of these films have revealed different in-plane lattice constants.³⁶ Thus we suggest the change of residual strain associated with the change in lattice constant value can account for the small difference in quadrupole splittings between the films.

E. Nonobservation of ODENDOR on the $g = 1.992$ deep defect

The nonobservation of ODENDOR on the ODMR feature with $g = 1.992$ is surprising and deserves some discussion. The line shape of this resonance is Gaussian, and is independent of microwave frequency. This usually indicates the presence of a non-negligible central hyperfine interaction (if the defect nucleus has $I > 0$) and/or strong ligand hyperfine interactions due to lattice nuclei. However, no signals were found on the $g = 1.992$ ODMR.

Two possible reasons are offered for the absence of signals. First, the effects of inhomogeneous strains on strong hyperfine interactions (i.e., a/h , $b/h \gg 1$ MHz) must be considered. As noted above, such strong interactions are anticipated for deep defects in III–V semiconductors. The random strain fields in these highly dislocated films can produce a spread of hyperfine interactions rather than a unique value. As a result, the ENDOR may be rendered unobservable due to severe broadening.

Second, rather than broadening due to an unresolved hyperfine interaction, the ODMR linewidth may reflect an unresolved fine-structure splitting that can arise from the defect having two or more electrons coupled together to give a total spin $> \frac{1}{2}$ and if the symmetry of the defect is lower than cubic (as expected for wurtzitic GaN or from a local distortion). This spin-spin interaction introduces higher-order terms in \mathbf{S} into the spin Hamiltonian. The most important of these terms is typically quadratic in \mathbf{S} with the form $\mathbf{S} \cdot \mathbf{D} \cdot \mathbf{S}$ (in favorable cases, $2S$ lines will be observed). Examples of defects with high electron spin include transition metals such as Fe and Cr and doubly occupied Ga_i or N_{Ga} .

VI. SUMMARY

Optically detected electron-nuclear double resonance has been performed on several GaN epitaxial layers. Searches were made on both the effective-mass donor and deep-defect ODMR on the 2.2-eV emission.

Strong ODENDOR with a resolved quadrupole structure assigned to neighboring $^{69,71}\text{Ga}$ lattice nuclei was found on the EM resonance from two high-resistivity GaN films. The main characteristics of these signals can be described using second-order perturbation theory for the quadrupole interaction. The observed splittings arise from the wurtzite structure perturbed by the local strain. No ODENDOR was found on the EM donor from two films with $n \geq 3 \times 10^{16} \text{ cm}^{-3}$.

Though more work needs to be done, these ODENDOR studies did not reveal signals on the ODMR feature assigned to deep states. Possible reasons for the lack of signals include (1) the effects of inhomogeneous strains on strong hyperfine interactions, and (2) the fact that the broadening of the ODMR is due to an unresolved fine-structure splitting rather than a hyperfine interaction.

The chemical identification of the residual shallow and deep defects in GaN epitaxial layers remains elusive. The observation of hyperfine interactions associated with group-IV (such as Si) and group-VI (such as O) impurities is problematic due to their low natural abundance of isotopes with $I > 0$ (i.e., 4.7% for ^{29}Si and 0.04% for ^{17}O). A deep state produced by e^- irradiation of GaN films has been identified from ODMR (Ref. 37) as a complex involving a Ga interstitial from a resolved hyperfine interaction. This result provides hope that further microscopic identifications of the residual defects in GaN layers will be achieved in the near future.

Finally, there is a strong prospect to determine the location of the residual donors in these GaN films from the sensitivity of the quadrupole splittings to the degree of local strain. It should be possible to differentiate between donors in the hexagonal crystallites and at grain boundaries.

ACKNOWLEDGMENTS

We would like to thank J.-M. Spaeth (Paderborn University), F. K. Koschnick (Paderborn University), S. W. Brown (NRL), and H. S. Newman (NRL) for many helpful discus-

sions and for the exchange of results prior to publication. We also thank S. C. Binari (NRL) for electrical transport and W. J. Moore (NRL) for infrared reflectivity measurements of some of the samples investigated in these studies. This work was supported by the Office of Naval Research.

- ¹D. C. Look, D. C. Reynolds, J. W. Hemsley, J. R. Sizelove, R. L. Jones, and R. J. Molnar, *Phys. Rev. Lett.* **79**, 2273 (1997).
- ²W. Götz, N. M. Johnson, D. P. Bour, C. Chen, H. Liu, C. Kuo, and W. Imler, in *Gallium Nitride and Related Materials*, edited by R. D. Dupuis, J. A. Edmond, F. A. Ponce, and S. Nakamura, MRS Symposia Proceedings No. 395 (Materials Research Society, Pittsburgh, 1996), p. 443, and references therein.
- ³See, for example, B. K. Meyer, in *III-V Nitrides*, edited by F. A. Ponce, T. D. Moustakas, I. Akasaki, and B. A. Monemar, MRS Symposia Proceedings No. 449 (Materials Research Society, Pittsburgh, 1997), p. 497, and references therein.
- ⁴M. Ramsteiner, A. J. Menniger, O. Brandt, H. Yang, and K. H. Ploog, *Appl. Phys. Lett.* **69**, 1276 (1996).
- ⁵W. E. Carlos, J. A. Freitas, Jr., M. Asif Khan, D. T. Olson, and J. N. Kuznia, *Phys. Rev. B* **48**, 17 878 (1993).
- ⁶N. M. Reinacher, H. Angerer, O. Ambacher, M. S. Brandt, and M. Stutzmann, in MRS Symposia Proceedings No. 449 (Materials Research Society, Pittsburgh, 1997), p. 579.
- ⁷E. R. Glaser, T. A. Kennedy, K. Doverspike, L. B. Rowland, D. K. Gaskill, J. A. Freitas, Jr., M. Asif Khan, D. T. Olson, J. N. Kuznia, and D. K. Wickenden, *Phys. Rev. B* **51**, 13 326 (1995), and references therein.
- ⁸U. Kaufmann, M. Kunzer, C. Merz, I. Akasaki, and H. Amano, in *Gallium Nitride and Related Materials* (Ref. 2), and references therein.
- ⁹D. M. Hofmann, D. Kovalev, G. Steude, D. Volm, B. K. Meyer, C. Xavier, T. Monteiro, E. Pereira, E. N. Mokov, H. Amano, and I. Akasaki, in *Gallium Nitride and Related Materials* (Ref. 2), p. 619.
- ¹⁰P. W. Mason, G. D. Watkins, and A. Dornen, in *III-V Nitrides* (Ref. 3), p. 793.
- ¹¹W. Qian, M. Skowronski, M. DeGraef, K. Doverspike, L. B. Rowland, and D. K. Gaskill, *Appl. Phys. Lett.* **66**, 1252 (1995).
- ¹²F. A. Ponce, B. S. Krusor, J. S. Major, Jr., W. E. Plano, and D. F. Welch, *Appl. Phys. Lett.* **67**, 410 (1995).
- ¹³S. D. Hersee, J. C. Ramer, and K. J. Malloy, *Mater. Res. Bull.* **22**, 45 (1997).
- ¹⁴S. Nakamura, T. Mukai, and M. Senoh, *Appl. Phys. Lett.* **64**, 1687 (1994).
- ¹⁵S. Nakamura, M. Senoh, S. Nagahama, N. Iwasa, T. Yamada, T. Matsushita, Y. Sugimoto, and H. Kiyoku, *Appl. Phys. Lett.* **70**, 1417 (1997).
- ¹⁶See, for example, D. Walker, X. Zhang, A. Saxler, P. Kung, J. Xu, and M. Razeghi, *Appl. Phys. Lett.* **70**, 949 (1997).
- ¹⁷M. A. Khan, J. N. Kuznia, D. T. Olson, W. Schaff, J. Burm, and M. S. Shur, *Appl. Phys. Lett.* **65**, 1121 (1994).
- ¹⁸S. Binari, L. B. Rowland, W. Kruppa, G. Kelner, K. Doverspike, and D. K. Gaskill, *Electron. Lett.* **30**, 1248 (1994).
- ¹⁹F. K. Koschnick, K. Michael, J.-M. Spaeth, B. Beaumont, and P. Gibart, *Phys. Rev. B* **54**, R11 042 (1996).
- ²⁰G. Denninger and D. Reiser, *Phys. Rev. B* **55**, 5073 (1997); G. Denninger, R. Beerhalter, D. Reiser, K. Maier, J. Schneider, T. Detchprohm, and K. Hiramatsu, *Solid State Commun.* **99**, 347 (1996).
- ²¹A. E. Wickenden, D. K. Gaskill, D. D. Koleske, K. Doverspike, D. S. Simons, and P. H. Chi, in *Gallium Nitride and Related Materials* (Ref. 2), p. 679, and references therein.
- ²²D. Y. Jeon, Ph. D. thesis, Lehigh University, 1988.
- ²³See, for example, J.-M. Spaeth, J. R. Niklas, and R. Bartram, in *Structural Analysis of Point Defects in Solids*, edited by H.-J. Queisser (Springer-Verlag, Berlin, 1992).
- ²⁴M. H. Cohen and F. Reif, *Solid State Phys.* **5**, 321 (1957).
- ²⁵J. A. Freitas, Jr., K. Doverspike, and A. E. Wickenden, in *Gallium Nitride and Related Materials* (Ref. 2), p. 485.
- ²⁶R. Dingle and M. Ilegems, *Solid State Commun.* **9**, 175 (1971).
- ²⁷E. R. Glaser, T. A. Kennedy, A. E. Wickenden, D. D. Koleske, and J. A. Freitas, Jr., in *III-V Nitrides* (Ref. 3), p. 543.
- ²⁸E. R. Glaser, T. A. Kennedy, A. E. Wickenden, D. D. Koleske, and J. A. Freitas, Jr. (unpublished).
- ²⁹*Semiconductors. Physics of Group IV Elements and III-V Compounds*, edited by K. H. Hellwege and A. M. Hellwege, Landolt-Börnstein, New Series, Group III, Vol. 31, Pt. a (Springer-Berlin, Berlin 1993).
- ³⁰B. Utsch, A. Igelmund, and A. Hausmann, *Z. Phys. B* **30**, 111 (1978); A. Igelmund, A. Hausmann, and B. Utsch, *ibid.* **32**, 265 (1979).
- ³¹J. J. Davies, J. E. Nicholls, and R. P. Barnard, *J. Phys. C* **18**, L93 (1985).
- ³²See, for example, J. E. Nicholls, J. J. Davies, B. C. Cavenett, J. R. James, and D. J. Dunstan, *J. Phys. C* **12**, 2927 (1979).
- ³³M. Godlewski, W. M. Chen, and B. Monemar, *Phys. Rev. B* **37**, 2570 (1988).
- ³⁴R. S. Title, *Phys. Rev.* **154**, 668 (1967).
- ³⁵O. H. Han, H. K. C. Timken, and E. Oldfield, *J. Chem. Phys.* **89**, 6046 (1988).
- ³⁶E. R. Glaser, T. A. Kennedy, A. E. Wickenden, D. D. Koleske, W. G. Perry, and R. F. Davis, in *Nitride Semiconductors*, edited by F. A. Ponce, S. P. Den Baars, B. K. Meyers, S. Nakamura, and T. Strite, MRS Symposia Proceedings No. 482 (Materials Research Society, Pittsburgh, in press).
- ³⁷Matthias Linde, S. J. Uffring, G. D. Watkins, V. Härle, and F. Scholz, *Phys. Rev. B* **55**, R10 177 (1997).